η Photoproduction on the Proton for Photon Energies from 0.75 to 1.95 GeV

M. Dugger,[1] B. G. Ritchie,[1] J. Ball,[1] E. Pasyuk,[1] G. Adams,[26] E. Anciant,[30] M. Anghinolfi,[14] B. Asavapibhop,[19] G. Audit,[30] T. Auger,[30] H. Avakian,[33,13] H. Bagdasaryan,[37] S. Barrow,[10] M. Battaglieri,[14] K. Beard,[17] M. Bektasoglu,[24] M. Bellis,[26] B. L. Berman,[11] N. Bianchi,[13] A. S. Biselli,[26] S. Boiarinov,[33,16] S. Bouchigny,[15] R. Bradford,[3] D. Branford,[8] W. J. Briscoe,[11] W. K. Brooks,[33] V. D. Burkert,[33] J. R. Calarco,[21] G. P. Capitani,[13] D. S. Carman,[23] B. Carnahan,[4] C. Cetina,[11] R. Clark,[3] P. L. Cole,[32,33] A. Coleman,[36] J. Connelly,[11] D. Cords,[33] P. Corvisiero,[14] D. Crabb,[34] H. Crannell,[4] J. P. Cummings,[26] E. DeSanctis,[13] R. DeVita,[14] P. V. Degtyarenko,[33,16] H. Denizli,[25] L. Dennis,[10] K. V. Dharmawardane,[24] K. S. Dhuga,[11] C. Djalali,[31] G. E. Dodge,[24] D. Doughty,[5,33] P. Dragovitsch,[10] S. Dytman,[25] M. Eckhause,[36] H. Egiyan,[36] K. S. Egiyan,[37] L. Elouadrhiri,[33,5] L. Farhi,[30] R. Fatemi,[34] G. Feldman,[11] R. J. Feuerbach,[3] J. Ficenec,[35] T. A. Forest,[24] V. Frolov,[26] H. Funsten,[36] S. J. Gaff,[7] M. Gai,[6] G. Gavalian,[21] S. Gilad,[20] G. P. Gilfoyle,[28] K. L. Giovanetti,[17] P. Girard,[31] C. I. O. Gordon,[12] K. Griffioen,[36] M. Guidal,[15] M. Guillo,[31] L. Guo,[33] V. Gyurjyan,[33] C. Hadjidakis,[15] D. Hancock,[36] J. Hardie,[5,33] D. Heddle,[5,33] P. Heimberg,[11] F. W. Hersman,[21] K. Hicks,[19] R. S. Hicks,[19] M. Holtrop,[21] C. E. Hyde-Wright,[24] M. M. Ito,[33] D. Jenkins,[35] K. Joo,[33,34] J. H. Kelley,[7] J. D. Kellie,[12] M. Khandaker,[22] W. Kim,[18] A. Klein,[24] F. J. Klein,[4,33] M. Klusman,[26] M. Kossov,[16] V. Koubarovski,[26] L. H. Kramer,[9,33] Y. Kuang,[36] S. E. Kuhn,[24] J. Kuhn,[26] J. Lachniet,[3] J. M. Laget,[30] D. Lawrence,[19,1] Ji Li,[26] K. Livingston,[12] A. Longhi,[4] M. Lucas,[31] K. Lukashin,[33] W. Major,[28] J. J. Manak,[33] C. Marchand,[30] S. McAleer,[10] J. McCarthy,[34] J. W. C. McNabb,[3] B. A. Mecking,[33] S. Mehrabyan,[25] M. D. Mestayer,[33] C. A. Meyer,[3] K. Mikhailov,[16] R. Minehart,[34] M. Mirazita,[13] R. Miskimen,[19] L. Morand,[30] S. A. Morrow,[15] M. U. Mozer,[23] V. Muccifora,[13] J. Mueller,[25] L. Y. Murphy,[11] G. S. Mutchler,[27] J. Napolitano,[26] R. Nasseripour,[9] S. O. Nelson,[7] S. Niccolai,[11] G. Niculescu,[23] I. Niculescu,[11] B. B. Niczyporuk,[33] R. A. Niyazov,[24] M. Nozar,[33] J. T. O'Brien,[4] G. V. O'Rielly,[11] A. K. Opper,[23] K. Park,[18] G. Peterson,[19] S. A. Philips,[11] N. Pivnyuk,[16] D. Počanić,[34] O. Pogorelko,[16] E. Polli,[13] S. Pozdniakov,[16] B. M. Preedom,[31] J. W. Price,[2,26] Y. Prok,[34] D. Protopopescu,[21] L. M. Qin,[24] B. A. Raue,[9,33] G. Riccardi,[10] G. Ricco,[14] M. Ripani,[14] F. Ronchetti,[13,29] P. Rossi,[13] D. Rowntree,[20] P. D. Rubin,[28] F. Sabatié,[30] K. Sabourov,[7] C. Salgado,[22] J. P. Santoro,[35,33] M. Sanzone-Arenhovel,[14] V. Sapunenko,[14] R. A. Schumacher,[3] V. S. Serov,[16] A. Shafi,[11] Y. G. Sharabian,[33,37] J. Shaw,[19] A. V. Skabelin,[20] E. S. Smith,[33] T. Smith,[21] L. C. Smith,[34] D. I. Sober,[4] M. Spraker,[7] A. Stavinsky,[16] S. Stepanyan,[24,37] P. Stoler,[26] I. I. Strakovsky,[11] S. Strauch,[11] M. Taiuti,[14] S. Taylor,[20,27] D. J. Tedeschi,[31,25] U. Thoma,[33] R. Thompson,[25] L. Todor,[3] M. Ungaro,[26] M. F. Vineyard,[28] A. V. Vlassov,[16] K. Wang,[34] L. B. Weinstein,[24] H. Weller,[7] D. P. Weygand,[33] C. S. Whisnant,[31] M. Witkowski,[26] E. Wolin,[33] M. H. Wood,[33] A. Yegneswaran,[33] J. Yun,[24] B. Zhang,[20] J. Zhao,[20] and Z. Zhou[20]

(CLAS Collaboration)

[1]*Arizona State University, Department of Physics and Astronomy, Tempe, Arizona 85287*
[2]*University of California at Los Angeles, Los Angeles, California 90095-1547*
[3]*Carnegie Mellon University, Pittsburgh, Pennsylvania 15213*
[4]*Catholic University of America, Washington, D.C. 20064*
[5]*Christopher Newport University, Newport News, Virginia 23606*
[6]*University of Connecticut, Storrs, Connecticut 06269*
[7]*Duke University, Durham, North Carolina 27708-0305*
[8]*Edinburgh University, Edinburgh EH9 3JZ, United Kingdom*
[9]*Florida International University, Miami, Florida 33199*
[10]*Florida State University, Tallahasee, Florida 32306*
[11]*The George Washington University, Washington, D.C. 20052*
[12]*University of Glasgow, Glasgow G12 8QQ, United Kingdom*
[13]*INFN, Laboratori Nazionali di Frascatti, Frascati, Italy*
[14]*INFN, Sezione di Genova, 16146 Genova, Italy*
[15]*Institut de Physique Nucleaire ORSAY, Orsay, France*
[16]*Institute of Theoretical and Experimental Physics, Moscow, 117259, Russia*
[17]*James Madison University, Harrisonburg, Virginia 22807*
[18]*Kyungpook National University, Daegu 702-701, South Korea*
[19]*University of Massachusetts, Amherst, Massachusetts 01003*
[20]*Massachusetts Institute of Technology, Cambridge, Massachusetts 02139-4307*
[21]*University of New Hampshire, Durham, New Hampshire 03824-3568*
[22]*Norfolk State University, Norfolk, Virginia 23504*

[23]Ohio University, Athens, Ohio 45701
[24]Old Dominion University, Norfolk, Virginia 23529
[25]University of Pittsburgh, Pittsburgh, Pennsylvania 15260
[26]Rensselaer Polytechnic Institute, Troy, New York 12180-3590
[27]Rice University, Houston, Texas 77005-1892
[28]University of Richmond, Richmond, Virginia 23173
[29]Universitá di Roma III, 00146 Roma, Italy
[30]CEA-Saclay, Service de Physique Nucléaire, F91191 Gif-sur-Yvette, Cedex, France
[31]University of South Carolina, Columbia, South Carolina 29208
[32]University of Texas at El Paso, El Paso, Texas 79968
[33]Thomas Jefferson National Accelerator Laboratory, Newport News, Virginia 23606
[34]University of Virginia, Charlottesville, Virginia 22901
[35]Virginia Polytechnic Institute and State University, Blacksburg, Virginia 24061-0435
[36]College of Willliam and Mary, Williamsburg, Virginia 23187-8795
[37]Yerevan Physics Institute, 375036 Yerevan, Armenia

Differential cross sections for $\gamma p \to \eta p$ have been measured with tagged real photons for incident photon energies from 0.75 to 1.95 GeV. Mesons were identified by missing mass reconstruction using kinematical information for protons scattered in the production process. The data provide the first extensive angular distribution measurements for the process above $W = 1.75$ GeV. Comparison with preliminary results from a constituent quark model support the suggestion that a third S_{11} resonance with mass ~1.8 GeV couples to the ηN channel.

Much effort is being directed at more fully understanding the internal structure of the proton and neutron. An important tool in this effort is the spectroscopy of their excited states, the N^* resonances. Results to date [1] have come from a variety of analyses of πN and γN experiments, including traditional Breit-Wigner fits [2,3] and more sophisticated global, unitary fits [4,5]. More recently, others have begun to use the measured N^* properties to probe the internal structure of the states in terms of constituent quarks. Such models explain a significant body of data in terms of quark effective degrees of freedom [6]. Additionally, full quantum chromodynamics calculations of N^* properties on a lattice are underway [7]. Although these methods describe many types of data, uncertainty about resonance properties and structure remain. An unambiguous understanding of the N^* resonances demands more extensive measurements.

The challenges presented in understanding nucleon structure are large, in part due to the complexity of this strongly interacting system and to the presence of many broad and overlapping resonances. Of particular interest in investigating nucleon structure, then, are probes that help isolate individual states and ascertain the importance of specific contributions. Since the electromagnetic interaction is so well understood, electromagnetic probes offer one of the more insightful methods for studying the nucleon. The photoproduction reaction $\gamma p \to \eta p$ is ideal in this regard, since the reaction provides an "isospin filter" to the nucleon response, as ηN final states can originate only from isospin $I = 1/2$ systems. While the $S_{11}(1535)$ nucleon resonance is known to dominate the reaction near threshold, measurements of the differential cross sections with broad coverage of scattering angle and center-of-mass energy W can provide insight into which other resonances couple to ηN final states. But in recent studies of η photo- and electroproduction [8–11], only two [10,11] were conducted at energies high enough to excite resonances with masses significantly above the region of the $S_{11}(1535)$ resonance. Furthermore, since nucleon resonances are wide ($\sim$ 100–300 MeV) and interfere with each other, more information concerning any higher mass resonances is needed even to understand the $S_{11}(1535)$ better. Finally, the existing data used for nucleon resonance searches are dominated by πN experiments. Poorly known resonances with small couplings to the πN channel might be seen more clearly in an ηN experiment.

We report here differential cross sections for $\gamma p \to \eta p$ for incident laboratory photon energies E_γ in 24 bins from $E_\gamma = 775 \pm 25$ to 1925 ± 25 MeV [12]. This photon energy range corresponds to W from 1.51 to 2.13 GeV, overlapping existing data and greatly extending coverage in W and $\cos\theta_{\text{c.m.}}$, where $\theta_{\text{c.m.}}$ is the meson scattering angle in the center of mass. The measurements were obtained with the CEBAF Large Acceptance Spectrometer (CLAS) [13,14] and the bremsstrahlung photon tagger [15] at the Thomas Jefferson National Accelerator Facility (Jefferson Lab). The energy of the electron beam impinging on the radiator of the photon tagger was 2.49 GeV. The event trigger required detection of a scattered electron in the photon tagger focal plane in coincidence with a charged particle detected in CLAS.

The tagged photon beam was incident on a liquid hydrogen target placed at the center of CLAS. This

cryogenic target, 18 cm in length, was enclosed by a scintillator array that detected the passage of charged particles into CLAS from the target [16]. This array, coupled with the time-of-flight array [17] of CLAS and accelerator radio-frequency information, allowed the velocity of the scattered charged particles to be determined. Tracking of the charged particles through CLAS by the drift chamber system [18] provided a determination of their momentum and scattering angle.

Photoproduced mesons were identified using the recoil proton information from CLAS to determine the missing mass, assuming the reaction $\gamma p \rightarrow pX$. Using this approach, multiple scattering of the recoil protons in the target and CLAS detector materials limited usable data for the reaction $\gamma p \rightarrow \eta p$ to photon energies above 750 MeV ($W = 1.51$ GeV) and center-of-mass scattering angles in the range $-0.8 \leq \cos\theta_{c.m.} \leq 0.8$. As seen in the missing mass spectrum in Fig. 1, the resolution obtained is sufficient to clearly identify the π^0, η, $\rho + \omega$, and η' meson peaks, the latter three peaks atop a multipion background. This same spectrum was binned in proton center-of-mass scattering angle and photon energy in order to extract yields for π^0, η, and η' mesons for each angle/energy bin. (While we report here cross sections for η meson photoproduction, results for η' will be presented elsewhere.) Background subtraction was performed assuming a mixture of two- and three-pion contributions [12]. This subtraction, an example of which is shown in the inset in Fig. 1, was unambiguous in all cases.

The proton detection efficiency for CLAS was measured empirically using the reaction $\gamma p \rightarrow p\pi^+\pi^-$ [12,19]. With this reaction, for a given set of momenta and angles for the two charged pions and a given incident photon energy, the proton momentum and scattering

angle are uniquely determined. With this kinematical information for the charged pions, a three-body final state missing mass reconstruction was used to determine if a proton should have been detected in CLAS in a particular spectrometer laboratory phase-space volume. The presence of a proton in that volume yielded an empirical measure of the momentum-dependent proton detection efficiency for that volume. Efficiency uncertainties, dominated by the statistical uncertainty in the number of protons scattered and detected in each phase-space bin, were determined for each bin, and were generally from $\sim 2\%$–3% at the lowest energies and to $\sim 6\%$–7% at the highest energies.

With these empirical detection efficiency measurements and the yields for each bin from the missing mass reconstruction for $\gamma p \rightarrow pX$, photoproduced π^0, η, and η' yields for each bin were converted into relative cross sections. Absolute normalization of these relative cross sections was performed by normalizing the measured relative cross sections for π^0 photoproduction to the SAID partial wave analysis parametrizations for pion photoproduction [4]. This SAID analysis incorporates many observables for all channels of pion photoproduction, and provides an estimated normalization uncertainty of 3% for all photon energies below 2 GeV. A fit of the measured relative differential cross sections for π^0 photoproduction at each energy to the SAID values yielded a single multiplicative constant establishing the absolute normalization at that energy. This same fit provided an additional check on the empirical CLAS detector response by comparison of the predicted SAID shape to the measured relative angular distribution; in all cases the comparison indicated the angular distributions were within uncertainties. Statistical uncertainties in the normalization arising from this single parameter fit were typically less than 3%. Combining this statistical uncertainty with an estimate of the uncertainty in the SAID parametrizations, overall normalization uncertainties were estimated to range from 3%–7%, rising with photon energy.

The resulting differential cross sections are shown in Figs. 2 and 3. Existing measurements at approximately the same E_γ from TAPS [8] and from GRAAL [11] are shown for comparison in Fig. 2. In general, agreement is very good. Since the cross section falls rapidly beyond the peak of the $S_{11}(1535)$ resonance, most differences in Fig. 2 between previous work and our results are likely due to small differences in incident photon energy.

To estimate total cross sections from these data, an extrapolation to unmeasured angular regions must be made. Such an extrapolation is very sensitive to the physics incorporated in modeling the reaction. An isobar model for η photo- and electroproduction (ETA-MAID) [3] was used here to guide the necessary extrapolation of our data to unmeasured angular regions. Reference [3] used the differential cross sections for η photoproduction
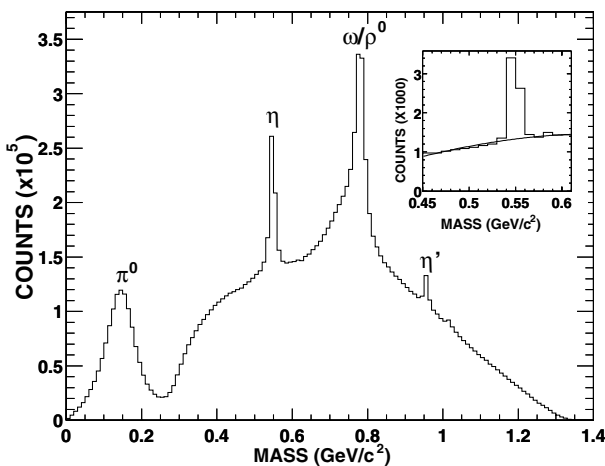

FIG. 1. Missing mass spectrum for $\gamma p \rightarrow pX$ for this experiment, summed over all energies and angles. Various meson peaks are indicated. Inset: Same spectrum binned in photon energy (0.875 ± 0.025 GeV) and angle ($0.0 \leq \cos\theta_{c.m.} \leq 0.2$), showing the background fit discussed in the text.
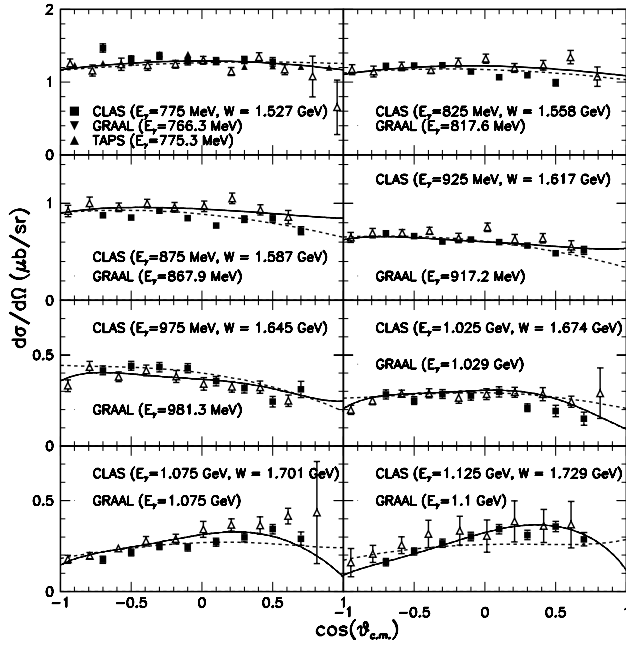
FIG. 2. Cross sections for $\gamma p \to p\eta$ reported here for photon energies from 775 ± 25 to 1125 ± 25 MeV. Statistical uncertainties are shown. Other results from TAPS [8] and GRAAL [11] are shown for comparison. Also shown are results from the REM [20] (solid line) and χQM [21] (dashed line) models.

reported in Refs. [8,11], polarization observable measurements on the same reaction [22], and electroproduction measurements reported in Refs. [9,10], to arrive at parameters for their multiple s-channel resonance model, which included contributions from Born terms and vector meson exchange. The data were described well using the $D_{13}(1520)$, $S_{11}(1535)$, $S_{11}(1650)$, $D_{15}(1675)$, $F_{15}(1680)$, $D_{13}(1700)$, $P_{11}(1710)$, and $P_{13}(1720)$ resonances, with values for masses and widths of the resonances in good agreement with accepted values [1].

For this work, the ETA-MAID fit has been performed again [20], with our differential cross sections added to the data set used previously. The preliminary results of this new fit are compared with our data in Figs. 2 and 3 (solid lines). This refit ETA-MAID model (REM) generally reproduces the shapes of the observed cross sections quite well, including the forward peak seen at the highest energies, usually interpreted to be due to t-channel processes. However, while the predicted shapes mimic those observed, the new calculations fall below the differential cross sections reported here around $W = 1.85$ GeV, and are above the data at $W \geq 1.9$ GeV.

Since the differential cross section shapes from REM are similar to those observed here, these shapes were used to approximate the differential cross section for regions beyond our angular coverage in order to make total cross section estimates σ_{est} at each photon energy. Each σ_{est} was obtained by first estimating contributions *outside* our angular coverage with the shape of the REM results,
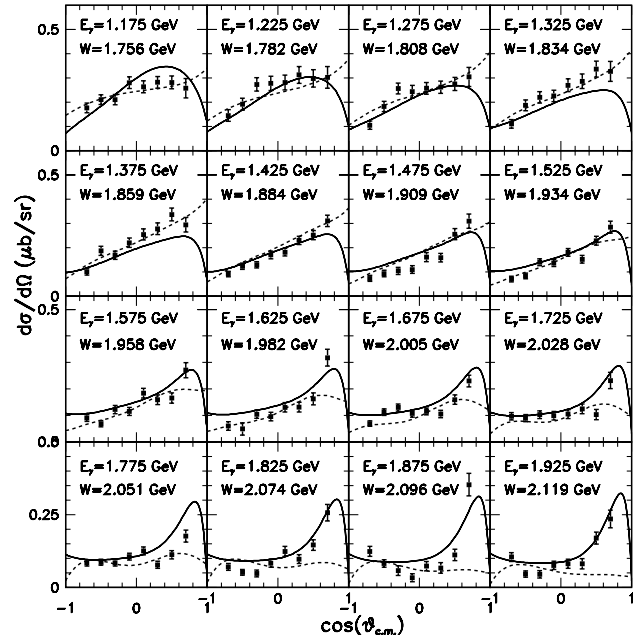

FIG. 3. Cross sections for $\gamma p \to p\eta$ reported in this work for photon energies from 1175 ± 25 to 1925 ± 25 MeV. Uncertainties and curves as in Fig. 2.

renormalized by a multiplicative constant to best fit our data exclusively at each energy. These contributions outside our measured region were then added to the sum of our measured differential cross sections to obtain σ_{est}, shown in Fig. 4. The statistical uncertainty shown in Fig. 4 is that for the measured contributions to σ_{est}. The systematic uncertainty shown is the combined normalization uncertainty noted above and the uncertainty in the multiplicative constant for the REM shape, assuming the shapes used accurately model the differential cross sections. The extrapolated portions of the angular distributions are 15%–30% of σ_{est}. In general, these estimates agree well with previous measurements, though they disagree significantly with the GRAAL published values at the highest energies reported there. Much of this discrepancy is due to the extrapolation procedure used in Ref. [11]. The agreement between the REM predications and these σ_{est} values is similar to the comparison noted above for the differential cross section, though the disagreement above $W = 1.75$ GeV is more apparent.

As noted above, attention has turned towards using quark-based approaches for understanding meson photo- and electroproduction. As an example, Saghai and Li [23,24] have used a chiral constituent quark model (χQM), based on an SU(6) ⊗ O(3) symmetry broken by gluon exchange interactions, to determine nucleon resonance quark wave functions and to study decays to various channels. Their approach has been applied to η photoproduction [23], using the set of resonances noted above in the ETA-MAID model and the $P_{11}(1440)$,
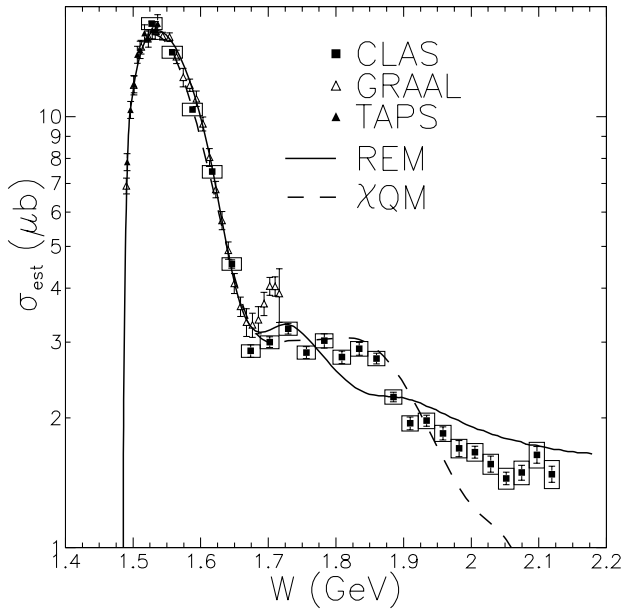
FIG. 4. Total cross section estimates from this work. Statistical uncertainties are indicated by error bars. Systematic uncertainties are represented by box height. Photon energy bin width is indicated by box width. Results from TAPS [8] and GRAAL [11] are shown for comparison. Curves as in Fig. 2.

$P_{13}(1900)$, and $F_{15}(2000)$ resonances. The data set investigated included the data used for the original ETA-MAID work, plus polarized target asymmetry data for η photoproduction from ELSA [25]. Good agreement with this data set was obtained, but the results were consistent with the broken $SU(6) \otimes O(3)$ symmetry only if an additional S_{11} resonance, not predicted by the quark model, was present at $W = 1.7$–1.8 GeV. A third S_{11} resonance near $W = 1.8$ GeV has been suggested by others [5,26,27], though the evidence is not strong. This resonance is near where the REM predictions fall below our data.

In preliminary calculations [21], the χQM has been extended to fit their original data set and our results. The resulting fit is shown in Figs. 2–4 (dashed curve). These preliminary results are generally in good agreement with data for $W \leq 1.9$ GeV. The inclusion of the third S_{11} resonance in these preliminary calculations, with a mass 1.79 GeV and width of 250–350 MeV, markedly improved the fit to our data [21]. The χQM agreement with our data around $W = 1.85$ GeV is considerably better than with the REM calculation, which lacks this third S_{11} resonance. (The agreement with σ_{est} would be even better had the χQM results been used to make the σ_{est} extrapolations rather than the REM predictions.) However, above $W = 1.9$ GeV, the χQM shapes are inconsistent with the peak at forward angles in the differential cross section as the energy increases. This disagreement

suggests, for instance, resonances in addition to those included in Ref. [23] may be needed, and t-channel contributions not incorporated directly in that model may also be important.

Our differential cross section data taken with the χQM predictions, thus, also provide hints of a third S_{11} resonance, with a mass near 1.8 GeV coupling to the ηN channel. However, a stronger case for that resonance must include simultaneous predictions of more observables for this reaction and other channels. Last, the failure of the χQM above 1.9 GeV to match our data here also provides evidence that resonances beyond those presently included in the χQM calculations may also couple to the ηN channel. More data on this process, including measurements of spin observables, are essential to resolving these issues.

[1]   D. E. Groom, et al., Eur. Phys. J. C **15**, 1 (2000).
[2]   For example, H. R. Hicks, S. R. Deans, D. T. Jacobs, P. W. Lyons, and D. L. Montgomery, Phys. Rev. D **7**, 2614 (1973); D. Drechsel, O. Hanstein, S. Kamalov, and L. Tiator, Nucl. Phys. **A645**, 145 (1999).
[3]   W.-T. Chiang, S. N. Yang, L. Tiator, and D. Drechsel, Nucl. Phys. **A700**, 429 (2002).
[4]   R. A. Arndt, W. J. Briscoe, I. I. Strakovsky, and R. L. Workman, nucl-th/0205067 [Phys. Rev. C (to be published)]; R. A. Arndt, I. I. Strakovsky, R. L. Workman, and M. M. Pavan, Phys. Rev. C **52**, 2120 (1995).
[5]   T. P. Vrana, S. A. Dytman, and T.-S. H. Lee, Phys. Rep. **328**, 181 (2000).
[6]   S. Capstick and W. Roberts, Prog. Part. Nucl. Phys. **45**, S241 (2000).
[7]   For example, S. V. Wright, D. B. Leinweber, A. W. Thomas, and K. Tsushima, Nucl. Phys. B (Proc. Suppl.) **109**, 50 (2002).
[8]   B. Krusche et al., Phys. Rev. Lett. **74**, 3736 (1995).
[9]   C. S. Armstrong et al., Phys. Rev. D **60**, 052004 (1999).
[10] R. Thompson et al., Phys. Rev. Lett. **86**, 1702 (2001).
[11] F. Renard et al., Phys. Lett. B **528**, 215 (2002).
[12] M. Dugger, Ph.D. dissertation, Arizona State University, 2001 (unpublished).
[13] W. K. Brooks, Nucl. Phys. **A663–A664**, 1077c (2000).
[14] B. A. Mecking et al. (to be published).

[15] D. I. Sober *et al.*, Nucl. Instrum. Methods Phys. Res., Sect. A **440**, 263 (2000).

[16] S. Taylor *et al.*, Nucl. Instrum. Methods Phys. Res., Sect. A **462**, 484 (2001).

[17] E. S. Smith, *et al.*, Nucl. Instrum. Methods Phys. Res., Sect. A **432**, 265 (199).

[18] M. D. Mestayer, *et al.*, Nucl. Instrum. Methods Phys. Res., Sect. A **449**, 81 (2000).

[19] T. Auger, Ph.D. dissertation, Université de Paris, 1999 (unpublished).

[20] W.-T. Chiang (private communication).

[21] B. Saghai, nucl-th/0202007.

[22] J. Ajaka, *et al.*, Phys. Rev. Lett. **81**, 1797 (1998).

[23] B. Saghai and Z. Li, Eur. Phys. J. A **11**, 217 (2001).

[24] Z. Li and B. Saghai, Nucl. Phys. **A644**, 345 (1998).

[25] A. Bock, *et al.*, Phys. Rev. Lett. **81**, 534 (1998).

[26] Z. Li and R. Workman, Phys. Rev. C **53**, R549 (1996).

[27] M. Batinić, *et al.*, Phy. Scr. **58**, 15 (1998).